Available online at www.sciencedirect.com
SCIENCE DIRECT®
Journal of Nuclear Materials 336 (2005) 156–162
journal of nuclear materials
www.elsevier.com/locate/jnucmat

High-dose neutron irradiation of $MgAl_2O_4$ spinel: effects of post-irradiation thermal annealing on EPR and optical absorption

A. Ibarra [a,*], D. Bravo [b], F.J. Lopez [b], F.A. Garner [c]

[a] EURATOM/CIEMAT Fusion Association, Inst. Investigación Básica, Av. Complutense, 22, E-28040 Madrid, Spain
[b] Departamento de Fisica de Materiales, Facultad de Ciencias (C-IV), Universidad Autonoma de Madrid, Cantoblanco, E-28049 Madrid, Spain
[c] Pacific Northwest National Laboratory, Richland, WA, USA

Received 1 March 2004; accepted 11 September 2004

Abstract

Electron paramagnetic resonance (EPR) and optical absorption spectra were measured during thermal annealing of stoichiometric $MgAl_2O_4$ spinel that was previously irradiated in the Materials Open Test Assembly in the Fast Flux Test Facility (FFTF/MOTA) at ≈680 K to ≈50 dpa. Both F and F^+ centres are to persist up to very high temperatures (over 1000 K) suggesting the operation of an annealing mechanism controlled by the thermal stability of extended defects. Using X-ray irradiation following the different annealing steps it was shown that an optical absorption band at 37000 cm^{-1} is related to a sharp EPR band at $g = 2.0005$ and that the defect causing these effects is the F^+ centre.

1. Introduction

$MgAl_2O_4$ is a ceramic spinel material with rather high radiation resistance for neutron irradiation, at least from the point of view of maintaining its original mechanical and elastic properties [1–5]. That resistance makes this material suitable for applications in intense radiation environments such as anticipated in fusion reactors. Other environments where $MgAl_2O_4$ could be useful are those which require a stable ceramic matrix such as in nuclear waste containment media [6,7] or as substrates for optical devices manufactured using ion implantation [8]. This resistance to radiation has been attributed to its structural characteristics, although the reason for this behaviour is not fully understood. Proposed mechanisms involve a very high recombination rate of radiation-induced point defects or a very difficult formation of dislocation loops. In any case, it seems to be related to an exceptional tolerance of this material toward a high concentration of intrinsic defects even in the absence of radiation.

One example of this tolerance is that up to 30% cation antisite disorder have been found to occur in synthetic spinel crystals, inducing a very high concentration of traps for electrons (Al^{3+} in tetrahedral symmetry sites) and holes (Mg^{2+} in octahedral symmetry sites) [9]. Another example is that $MgAl_2O_4$ crystals always exhibit

* Corresponding author. Tel.: +34 1 3466507; fax: +34 1 3466068.
E-mail address: angel.ibarra@ciemat.es (A. Ibarra).

0022-3115/$ - see front matter © 2004 Elsevier B.V. All rights reserved.
doi:10.1016/j.jnucmat.2004.09.003

some significant deviation from stoichiometry, i.e. the composition can be described as $(MgO)(Al_2O_3)_x$ with $x \geqslant 1.0$. Thus cation vacancies, mainly of tetrahedral type, are formed to maintain the spinel crystal structure [10]. After high-dose neutron irradiation it has been observed that the nucleation and growth of defect clusters is greatly inhibited, whereas the number of antisite defects increases enormously, in sharp contrast to the radiation response observed in other ceramic oxides [2,11–13].

The present work is a continuation of an experimental series in which an extensive characterization was performed on stoichiometric $MgAl_2O_4$ spinel specimens that were irradiated at high temperatures to very high neutron exposures (50–200 dpa) in the Materials Open Test Assembly in the Fast Flux Test Facility (FFTF/MOTA). In previous work the effect of irradiation temperature and total dose on stoichiometric spinels has been studied, with emphasis on point defects characteristics, using characterization techniques such as optical absorption, photoluminescence, electron paramagnetic resonance, electrical conductivity and others [14–16]. These specimens have also been characterized using neutron diffraction [12], as well as mechanical and elastic properties [3,4] and electron microscopy [9,17].

Before neutron irradiation, these samples do not present any EPR signal whereas the optical absorption spectra show some small bands (a few cm^{-1} intensity) in the UV region, related to residual impurities. After neutron irradiation, it has been observed a large increase in the optical absorption, mainly in the UV–VIS range as well as in some EPR bands. Generally speaking, the optical absorption increases in intensity with dose and decreases with increasing irradiation temperature [11,12]. To gain more information about the details of these radiation-induced changes, it is desirable to study the annealing behaviour of the radiation effects as a function of temperature. In particular, we report in this paper the results of a detailed study of annealing effects on both the optical absorption and electron paramagnetic resonance (EPR) spectra. The motivation for this work is to better understand the dynamic behaviour of point defects in $MgAl_2O_4$ to improve the knowledge of the behaviour of this material under irradiation, trying to clarify the origin of its radiation resistance.

2. Experimental details

The specimen studied was [1 0 0] oriented stoichiometric spinel single crystal from Union Carbide Corporation, in the form of a 4.8 mm diameter cylinder. The details of impurity levels, specimen fabrication and irradiation are given in [3]. The specimen was irradiated in the FFTF/MOTA facility at a nominal temperature of 680 K to a total fluence of 5.3×10^{26} n/m^2 ($E > 0.1$ MeV), producing ≈50 dpa. After irradiation, thin slices with thickness between 0.2 and 0.5 mm were cut and polished from the cylinder. The specimen was heated to 580 K to release all charges retained in shallow traps.

Optical absorption measurements were made at room temperature with a Cary 5E spectrometer between 3300 and 200 nm. EPR spectra were obtained with a Bruker spectrometer model ESP 300E working in the X-band. Accurate values of the microwave frequencies and magnetic fields were obtained with a Hewlett–Packard HP5342A frequency meter and a Bruker ER35 M gaussmeter, respectively. All spectra were measured with a modulation frequency of 100 kHz and modulation amplitude of 5×10^{-5} T.

Low dose X-ray irradiations were performed at room temperature through a 1 mm thick aluminium plate at about 0.5 Gy/s with a Siemens Kristalloflex 2H (tungsten anode) operated at 50 kV and 30 mA. The purpose of these irradiations was to assist in the identification of the defect types created by neutron irradiation. These X-ray irradiations were made in the neutron irradiated sample following the irradiation as well as after each annealing step of the neutron irradiated specimen.

Annealing was performed in air, using a conventional air-cooled oven able to reach 1200 °C. The ramp rate up to the maximum temperature and down to room temperature is 10 °C/min. The stabilization time at high temperature was ≈30 min.

3. Results and discussion

3.1. Optical absorption measurements

Fig. 1 shows the optical absorption spectra obtained after annealing different temperatures. Before the first annealing step, the observed spectrum shows very high absorption for energies over 34 000 cm^{-1} (4.22 eV) and a peak at around 19 500 cm^{-1} (2.42 eV). These results are in close agreement with those of previous studies [14].

The first annealing step was made at a temperature around 665 K, close to the nominal neutron irradiation temperature of 680 K. No annealing effect was expected at temperatures lower than the irradiation temperature. As can be observed in Fig. 1, increasing the annealing temperature from 665 to 1035 K induces a significant decrease in the magnitude of the optical absorption spectra, but the decrease is not uniform for all wavelengths. Clearly, it can be observed that the intensities at absorption energies below 46 000 cm^{-1} anneal out faster than those in the deep UV range.

During annealing it is possible to observe that the measured optical absorption spectra are related to the

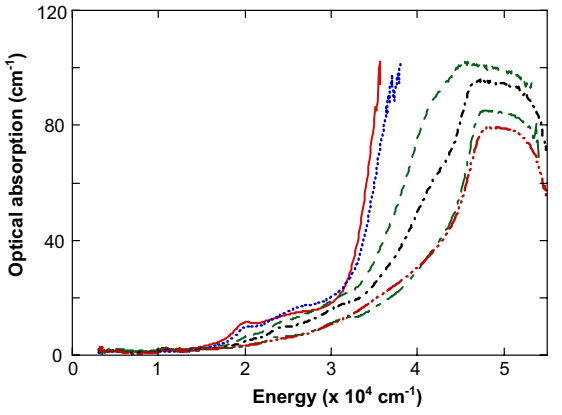

Fig. 1. Room-temperature optical absorption spectra of neutron-irradiated $MgAl_2O_4$ annealed at different temperatures: 675 K (solid line), 800 K (dotted line), 880 K (dashed line), 925 K (dot-dashed line), 970 K (dot-long dashed line) and1035 K(triple dot-dashed line).

presence of a number of different absorption bands. From the latter annealing steps in Fig. 1, it is possible to clearly identify the presence of a complex band in the 48 000–50 000 cm^{-1} (5.95–6.2 eV) region. Some additional components also seem to be present in the 35 000–45 000 cm^{-1} range. To improve the visibility of these latter bands, Fig. 2 shows the difference spectra between the different annealing steps and the final step (after annealing at 1035 K). This figure allows us to identify those optical absorption bands that are modified by the annealing process. The main annealing effect is related to the decrease of the intensity of a band around

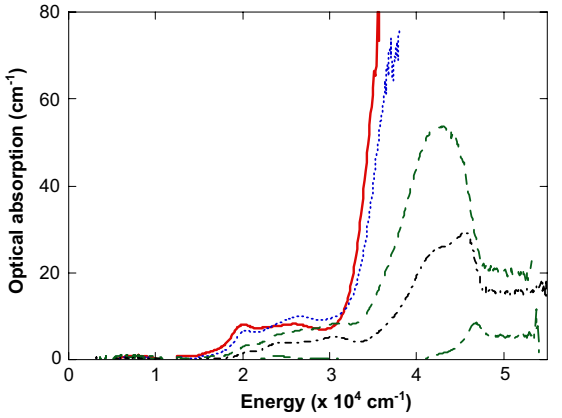

Fig. 2. Difference between the optical absorption spectra of neutron-irradiated $MgAl_2O_4$ annealed at different temperatures and the spectrum obtained after the 1035 K annealing: 675 K (solid line), 800 K (dotted line), 880 K (dashed line), 925 K (dot-dashed line) and 970 K (dot-long dashed line).

42 000 cm^{-1} (5.21 eV). In addition, annealing of optical absorption bands at 19 500 (2.42 eV), 28 000 (3.47 eV) and 46 000 cm^{-1} (5.70 eV) was also observed.

For temperatures higher than 1035 K, the specimen surface was degraded by reaction with the inner materials of the oven (mainly some kind of alumina), developing a white coating at the surface that precludes further optical measurements. This coating is now under study.

It is interesting to note that the band at 42 000 cm^{-1} has been also observed in neutron irradiated samples at lower doses and room temperature [18–21]. This band has been related to the presence of F centres. Bands at 27 000 cm^{-1} and 18 800 cm^{-1} were also observed in these studies. These bands can be considered to be similar to those observed in this current work at 28 000 and 19 500 cm^{-1}, especially taking into account the fact that they are complex bands probably associated with defects with slightly different distorted surroundings [20, 22 and 23]. In the case of very high-dose and high-temperature irradiation, it seems reasonable to assume that these bands can appear at slightly different positions.

From comparison of spectra in this work with those in [18], it is quite clear that the relative height of the UV absorption compared with the one at 19 500 cm^{-1} is very similar, whereas the height of the bands in the region around 25 000–30 000 cm^{-1} are quite different. This suggests that the dose and temperature dependences of the 19 500 cm^{-1} band and the UV absorption are similar, whereas the intensities of the other bands saturate at much lower doses.

Therefore, it seems that the defect responsible for absorption at 19 500 cm^{-1} is related to the defect responsible for the main UV absorption. It is also possible to observe that the annealing of the band at 19 500 cm^{-1} appears before the F centre annealing step since this band was not detected after the 885 K annealing. This behaviour is also observed in the annealing process described in [18] but at a completely different temperature (in this work the 18 800 cm^{-1} band is only observed below 730 K). Again this suggests that the band at 19 500 cm^{-1} is closely related to the UV bands. Taking into account that the UV bands are related to the oxygen vacancy defects (mainly F centres) it seems reasonable to relate the 19 500 cm^{-1} band to some oxygen vacancy defect, probably small clusters of two or three vacancies (giving rise to F_2 or F_3 defects). This proposal is further supported when taking into account that these type of defect also appears in the same energy region for Al_2O_3 or MgO [22,24], and that they anneal out before the main F centre annealing step.

At this point, it is important to note that these results suggest the presence of F centres in the irradiated material up to temperatures of 1000 K. This is considered to be a very high temperature for stable F centres. For low-dose and low-temperature irradiations it has been found

that optical bands related to V-centres anneal out for temperatures below 575 K [20,25–27], whereas bands related to F centres usually anneal out below 800 K [18,20,26]. Similar results have been observed for annealing of damage produced in low-dose, low-temperature irradiations using electrons [28]. Measurements of the vacancy centres during annealing made using other techniques such as positron annihilation [28] or length change [29] also provide similar information.

On the other hand, the annealing of specimens after high-dose, high-temperature irradiation shows a different behaviour. Unfortunately, for these irradiation conditions there are no corresponding optical data, but from transmission electron microscopy studies it was observed that radiation-induced dislocation loops start to shrink around 1000 K and completely disappear at 1500 K, whereas cavities grow slightly around 1600 K and then begin to shrink with increasing annealing temperature [17].

For other irradiation conditions, such as high-dose, low-temperature irradiation, there are no neutron data, but some qualitative information can be obtained by analysing ion implantation results. In this case, the thermal annealing of radiation damage for 60 keV Cu^- ion-implanted materials reaching the amorphization level shows that the crystallinity of the specimen recovers in a wide step starting at around 875 K, and almost fully recovers by 1500 K [8]. This recovery behaviour has been previously ascribed to the dissociation of defect clusters.

From these observations it can be concluded that in low-dose irradiations, vacancy centres in $MgAl_2O_4$ anneal out below 775 K in a process regulated by the mobility of point defects, whereas in high-dose irradiations, vacancy-related centres (such as the F centre) can be observed at very high temperatures and their thermal stability is controlled by the thermal stability of defect clusters.

As previously mentioned, data presented in Fig. 1 allow us to identify a complex band around 48 000–50 000 cm^{-1} that anneals out at even higher temperatures. Bands in this region have been previously observed after low-temperature and low-dose neutron irradiations [30] and after UV illumination [26,31], although they have not been related to any specific defect. It is interesting to note that the annealing behaviour observed is, again, similar to the one observed for the F centre bands. In this work the annealing takes place at high temperature (over 1000 K) whereas in the case of low-temperature and low-dose irradiations it appears below 650 K [30].

In summary, optical absorption spectrum changes induced by high-dose and high-temperature irradiation are composed of absorption bands at 48 000–50 000, 46 000, 42 000, 28 000 and 19 500 cm^{-1}. These bands anneal out at different temperatures in the range between 725 K and 1000 K or perhaps even higher.

3.2. EPR results

The EPR spectra at room temperature of the irradiated specimen before the first annealing step consists of a band at $g = 2.0005 \pm 0.0005$, as can be seen in Fig. 3. This band does not show any dependence on the orientation of the magnetic field with respect to the specimen. The band is sharp, with a peak-to-peak width of 1.1×10^{-3} T in the derivative line. These results are in agreement with those previously published [16]. It has been pointed earlier that this band could be related to F^+ centres [16,23].

During annealing, the height of this band decreases with temperature, almost disappearing after the last heat treatment. Fig. 4 shows the height of the measured band as a function of temperature. It is interesting to note that the decrease of the band takes place over the entire temperature range, and the observed behaviour is similar to that observed for the 42 000 cm^{-1} absorption band.

3.3. Ionizing radiation effects

It is well know that both optical absorption or EPR spectra are sensitive to the ionic and electronic configuration of point defects. Thus, the annealing of an optical or EPR band can be related to ionic annealing, in which the defect disappears by recombination, or to electronic annealing, in which the optical signature disappears (for example, by releasing or trapping an electron) but the ionic component of the defect is retained. So, in order to determine if the observed annealing behaviour is related to ionic or electronic effects, the samples were irradiated with X-rays after each annealing step, and the EPR and optical absorption properties were then

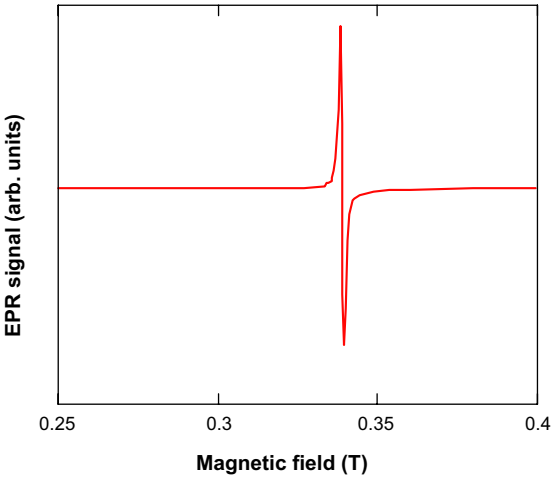

Fig. 3. Typical EPR spectrum at room temperature of the neutron-irradiated $MgAl_2O_4$ specimen.

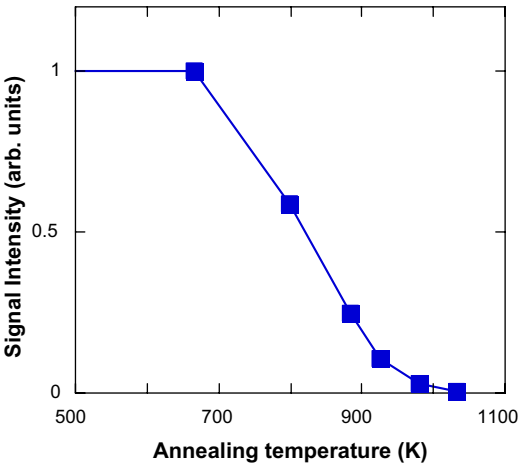

Fig. 4. Dependence of the EPR band intensity on annealing temperature on the neutron-irradiated $MgAl_2O_4$ specimen.

measured both before and after the X-ray irradiation. This subsequent X-radiation experiment generates a lot of electron–hole pairs that allow rearrangement of the defects charge state.

After neutron irradiation and before thermal annealing, no change of the spectra was found if a small level of X-ray irradiation was applied to the specimen. This is a very interesting result because before neutron irradiation, X-ray irradiation gives rise to very characteristic and intense EPR spectra associated with the trapping of holes in cation vacancies (V-centres) [26]. The lack of this band in the optical and EPR spectra of neutron-irradiated specimens should indicate that there are no cation vacancies available, although this is unlikely taking into account that their concentration is very high even in the starting material, or that these vacancies are distorted in such a way that they cannot stabilize the holes at the cation sites. A similar mechanism has been suggested to explain the higher sensitivity to gamma irradiation of stoichiometric single crystals compared with non-stoichiometric ones [30]. This proposal is further supported by the results obtained for other neutron irradiations at lower doses and lower temperatures in which it has been observed that characteristics of the optical and EPR spectra related to V centres are distorted by the irradiation and can be recovered after thermal annealing [18]. Most importantly, it should be noted that no recovery was observed in our case.

For X-ray irradiations made after annealing over 800 K an increase of the absorption spectra was clearly observed. In this case, as well as all the other annealing steps at higher temperatures, the dose dependence and the low-temperature annealing of the ionizing radiation effect have been studied. That means the experiment that was made consist of the following steps:

(i) Thermal heating up to a T_N temperature to partially anneal out neutron irradiation damage.
(ii) Several low-dose X-ray irradiations, to obtain the dose dependence of the ionizing radiation effect.
(iii) Several thermal heating steps up to different temperatures, much lower than T_N, to obtain the thermal annealing dependence of the ionizing radiation effect.
(iv) Repeat the cycle after a higher T_N.

In general, an increase of the optical absorption was measured, mainly in the region around 37 000 cm^{-1} (4.59 eV) and also around 19 000 cm^{-1} as a consequence of the X-ray irradiation. Fig. 5 shows the increase of the optical (i.e. the difference between the optical absorption spectra after and before X-ray irradiation) for the 880 K annealing step. At the same time, it is observed that the previously mentioned EPR band also increases after X-ray irradiation. Fig. 6 shows the dose dependence of both processes for the optical absorption at 37 000 cm^{-1} and for the EPR band. The observed increase in optical absorption and EPR bands anneals out at temperatures below 650 K in a wide annealing step process that starts at room temperature and finishes around 650 K, similar to the annealing behaviour observed for V-centres [22]. Fig. 7 shows the temperature dependence of this annealing, again for the optical absorption at 37 000 cm^{-1} and for the EPR band. Both bands behave in a similar way, indicating that they are related. In many papers this optical band has been assigned to F^+ centres [18–27]. Taking this relationship into account, it can be clearly concluded, for the first time, that the measured EPR band must be assigned with F^+ centres. These results also indicate the presence of oxygen vacancies at these temperatures, further demonstrating their high thermal stability.

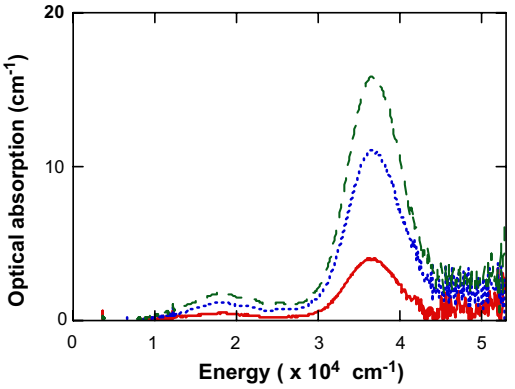

Fig. 5. Effects of different X-ray irradiations on the optical absorption spectra of a neutron-irradiated $MgAl_2O_4$ specimen annealed at 880 K: 0.3 kGy (solid line), 1.3 kGy (dotted line) and 3.3 kGy (dashed line).

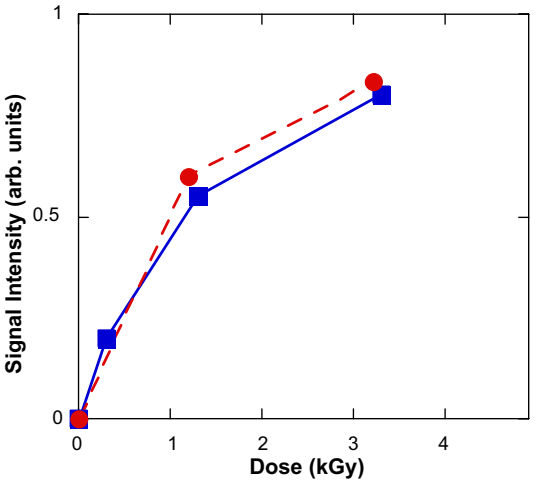

Fig. 6. Dose dependence of the X-ray effect of a neutron-irradiated $MgAl_2O_4$ specimen annealed at 880 K: (■) behaviour of the optical absorption band at 37000 cm^{-1}, (●) behaviour of the EPR band.

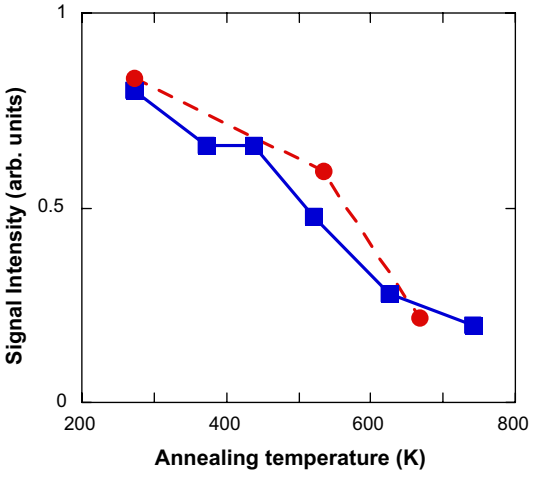

Fig. 7. Thermal annealing of the X-ray effect of a neutron-irradiated $MgAl_2O_4$ specimen annealed at 880 K: (■) behaviour of the optical absorption band at 37000 cm^{-1}, (●) behaviour of the EPR band.

4. Conclusions

Thermal annealing of the EPR and optical absorption characteristics of a $MgAl_2O_4$ specimen neutron-irradiated to 50 dpa at ≈680 K was studied. It was found that the main characteristics of EPR spectrum and some bands of the optical absorption spectra anneal out between 680 and 1100 K. Both F and F^+ centres were found to persist up to very high temperatures (over 1000 K), suggesting their thermal stability is controlled by the thermal stability of defect clusters. It has also been demonstrated, that a sharp EPR band with $g = 2.0005$ in these irradiated specimens is related to the presence of F^+ centres.

Acknowledgments

This work was performed in the framework of CIEMAT projects for Nuclear Fusion Research and was partly supported by the CICYT (Spain) under contract number FTN2003–03855. The neutron irradiation and the participation of F.A. Garner were performed under the sponsorship of the US Department of Energy, Office of Fusion Energy under Contract DE-AC06-76RLO 1830.

References

[1] F.W. Clinard Jr., G.F. Hurley, R.A. Youngman, L.W. Hobbs, J. Nucl. Mater. 133&134 (1985) 701.
[2] S. Zinkle, C. Kinoshita, J. Nucl. Mater. 251 (1997) 200.
[3] F.A. Garner, G.W. Hollenberg, F.D. Hobbs, J.L. Ryan, Z. Li, C.A. Black, R.C. Bradt, J. Nucl. Mater. 212–215 (1994) 1087.
[4] C.A. Black, F.A. Garner, R.C. Bradt, J. Nucl. Mater. 212–215 (1994) 1096.
[5] E.A.C. Neeft, R.J.M. Konings, K. Bakker, J.G. Boshoven, H. Hein, R.P.C. Sohram, A. van Veen, R. Conrad, J. Nucl. Mater. 274 (1999) 78.
[6] F.C. Klaassen, K. Bakker, R.P.C. Schram, R. Klein Meulekamp, R. Conrad, J. Somers, R.J.M. Konings, J. Nucl. Mater. 319 (2003) 108.
[7] T. Wiss, R.J.M. Konings, C.T. Walker, H. Thiele, J. Nucl. Mater. 320 (2003) 85.
[8] C.G. Lee, Y. Takeda, N. Kishimoto, Nucl. Instrum. and Meth. B 191 (2002) 591.
[9] R.I. Sheldom, T. Hartmann, K.E. Sickafus, A. Ibarra, D.N. Argyriou, A.C. Larson, R.B. von Breele, J. Am. Ceram. Soc. 82 (1999) 3293.
[10] T. Soeda, S. Matsumura, C. Kinoshita, N.J. Zaluzec, J. Nucl. Mater. 283–287 (2000) 952.
[11] K. Fukumoto, C. Kinoshita, F.A. Garner, J. Nucl. Sci. Technol. 32 (1995) 773.
[12] K.E. Sickafus, A.C. Larson, N. Yu, M. Nastasi, G.W. Hollenberg, F.A. Garner, R.C. Bradt, J. Nucl. Mater. 219 (1995) 128.
[13] K.E. Sickafus, N. Yu, M. Nastasi, Nucl. Instrum. and Meth. B 116 (1996) 85.
[14] A. Ibarra, R. Vila, F.A. Garner, J. Nucl. Mater. 233–237 (1996) 1336.
[15] A. Ibarra, F.A. Garner, G.L. Hollenberg, J. Nucl. Mater. 219 (1995) 135.
[16] A. Ibarra, D. Bravo, M.A. Garcia, J. Llopis, F.J. Lopez, F.A. Garner, J. Nucl. Mater. 258–263 (1998) 1902.
[17] K. Yasuda, C. Kinoshita, F.A. Garner, J. Nucl. Mater. 283–287 (2000) 937.

[18] A. Ibarra, D. Bravo, F.J. Lopez, I. Sildos, Mater. Sci. Forum 239–241 (1997) 595.
[19] G.P. Summers, G.S. White, K.H. Lee, J.R. Crawford Jr., Phys. Rev. B 21 (1980) 2578.
[20] L.S. Cain, G.J. Pogatshnik, Y. Chen, Phys. Rev. B 37 (1988) 2645.
[21] V.T. Gritsyna, I.V. Afanasyev-Charkin, V. Kobyakov, K.E. Sickafus, J. Nucl. Mater. 283–287 (2000) 927.
[22] M.J. Springis, J.A. Valbis, Phys. Stat. Sol. (b) 132 (1985) K61.
[23] V.T. Gritsyna, V. Kabyakov, Sov. Phys. Techn. Phys. 30 (1985) 206.
[24] L.S. Welch, A.E. Hughes, G.P. Pells, J. Phys. C: Solid State Phys. 13 (1980) 1805.
[25] V.T. Gritsyna, I.V. Afanasyev-Charkin, V. Kobyakov, K.E. Sickafus, J. Am. Ceram. Soc. 82 (1999) 3365.
[26] A. Ibarra, F.J. Lopez, M. Jimenez de Castro, Phys. Rev. B 44 (1991) 7256.
[27] G.S. White, K.H. Lee, J.R. Crawford Jr., Appl. Phys. Lett. 35 (1979) 1.
[28] J. He, L. Lin, T. Lu, P. Wang, Nucl. Instrum. and Meth. B 191 (2002) 596.
[29] T. Yano, A. Insani, H. Sawada, T. Iseki, J. Nucl. Mater. 258–263 (1998) 1836.
[30] N. Mironova, V. Skvortsova, A. Smirnov, U. Ulmanis, Sov. Phys. Solid State 34 (1992) 1492.
[31] V.T. Gritsyna, I.V. Afanasyev-Charkin, Yu.G. Kazarinov, K.E. Sickafus, Nucl. Instrum. and Meth. B 218 (2004) 264.